Int. J. Electrochem. Sci., 7 **(2012)** 7098 - 7110

International Journal of
ELECTROCHEMICAL
SCIENCE
www.electrochemsci.org

Effect of Stress on the Electrochemical Corrosion Behavior of Mg-Zn-In-Sn Alloy

Zhan YU[1], *Dongying JU*[2, 3, *], *Hongyang ZHAO*[3]

[1] Graduate School of Saitama Institute of Technology, Fusaiji 1690, Fukaya, Saitama 369-0293, Japan
[2] Department of Material Science and Engineering, Saitama Institute of Technology, Fusaiji 1690, Fukaya, Saitama 369-0293, Japan
[3] Department of Material Science and Engineering, University of Science and Technology Liaoning, Anshan 114051, China
[*]E-mail: dyju@sit.ac.jp

Received: 3 June 2012 / *Accepted:* 11 July 2012 / *Published:* 1 August 2012

Effects of stress on the electrochemical corrosion behaviours of Mg-Zn-In-Sn alloy anode were evaluated. Open circuit potential (OCP), loop current (LC) measurements, scanning electron microscopy (SEM) and electron probe micro-analysis (EPMA) analyses were used to investigate electrochemical properties, corrosion surface and cross section characteristics of alloy anodes. The results show that OCPs of Mg-Zn-In-Sn alloy anode are negatively removed and the LCs increase by stresses. Corrosion product films of alloy anodes are easy to shed off and the thicknesses of films decrease with increasing of stresses. LC calculation results are in almost agreement with those obtained by measurements. By adjusting the Tafel factors, the calculated results of LC were mainly consistent with the experimental results. The infuence of stresses on the LCs was revealed on the theoretial.

Keywords: Mg-Zn-In-Sn alloy; Stress; Electrochemical corrosion behavior

1. INTRODUCTION

Magnesium (Mg) alloys are useful because of their low density, high specific strength, good heat dissipation, good damping, and good electro-magnetic shield abilities [1]. The employment of Mg alloys as an anodic material in different types of batteries has been the subject of much attention in recent years. Mg alloys offer several advantages as negative electrode materials [2]. We have recently developed a new Mg alloy anode material called Mg-Zn-In-Sn alloy by adding the elements Zn, In and Sn into commercial Mg alloy AZ91 [3]. Mg-Zn-In-Sn alloy anode has more negative OCP and higher LC than those of AZ91 alloy because of the addition of elements. The OCP of AZ91 alloy is only

approximately -1.4 V vs. SHE, and the OCP of Mg-Zn-In-Sn alloy is approximately -1.5 V vs. SHE in 3.5 % sodium chloride (NaCl) solution. However, this value is still very different from the theoretical electrochemical potential of Mg (E_0 = -2.37 V vs. SHE). With the development of the electrochemical reaction of alloy anode, its potentials positively remove and currents decrease with the gradual thickening of the corrosion product film. Therefore, the current study aims to improve and maintain the electrochemical properties of Mg-Zn-In-Sn alloy anode. The application of stress accerelate the electrochemical corrosion of Mg alloys, due to improving the electrochemical activities of alloy. Therefore, Bonora et al. studied the corrosion behaviour of stressed Mg alloys [4]. Walke et al. studied corrosion resistance of AZ31 alloy after plastic working in NaCl solutions [5]. Furthermore, Eliezer studied corrosion behaviour of surfaced AM50 Mg alloys under stress condition [6]. The aforementioned studies prove the large interest in the improvements of electrochemistry properties of Mg alloys with stresses. In the present paper, effects of stress on OCPs and LCs of Mg-Zn-In-Sn alloy anode are investigated under electrochemical corrosion. After electrochemical measurements with stresses, the surface and cross section morphologies observation, and element distribution analyses of Mg-Zn-In-Sn alloy are investigated to reveal the correlation of stress and electrochemical properties of alloy anode. Finally, Tafel factors are investigated to confirm the influence of stress on the electrochemical properties of alloy anode through current curve calculation.

2. EXPERIMENTAL

2.1 Materials

Mg-Zn-In-Sn alloy was manufactured by adding metal elements Zn (1 wt.%), In (2 wt.%), and Sn (2 wt.%) in AZ91 alloy, which feature higher mechanical properties and electrochemical properties than that of AZ91 alloy [3, 7]. The alloy was cast via the twin-roll continuous casting method. The chemical composition of Mg-Zn-In-Sn alloy is shown in Table 1. And then alloy sheet was warm rolled to 0.5 mm thickness and annealed at 400 °C for 1 h. Specimens made of Mg-Zn-In-Sn alloy sheets by a wire cutting apparatus (Mitsubishi Electric Corporation W11FX2K) were used in the tensile tests and electrochemical measurements as presented in Fig. 1.

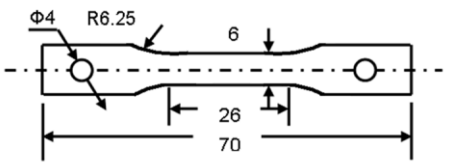

Figure 1. Schematic diagram of tensile test and stress corrosion specimen (unit: mm)

In order to provide electrical isolation between the surface of alloy anode and chuck of tensile tester, in our experiments, the clamped part of specimen was designed to open a hole with a diameter of 4 mm, and the acrylic resin sheets were fixed on both sides of specimen using a screw.

Table 1. Chemical analyses of Mg-Zn-In-Sn alloy

Material	Chemical analyses, wt %						
	Al	Zn	In	Sn	Mn	Other total	Mg
Mg-Zn-In-Sn alloy	10.161	0.776	0.877	1.847	0.268	0.138	balance

2.2 Tensile test and electrochemical measurement

The tensile tests using a tensile tester (Shimatsu Autograph AG-300KNG) were performed in the rolling and transverse directions with a speed of 7.8 mm/min (i.e., strain rate 5×10^{-3} /s at room temperature).

The schematic of stress corrosion apparatus is as shown in Fig. 2.

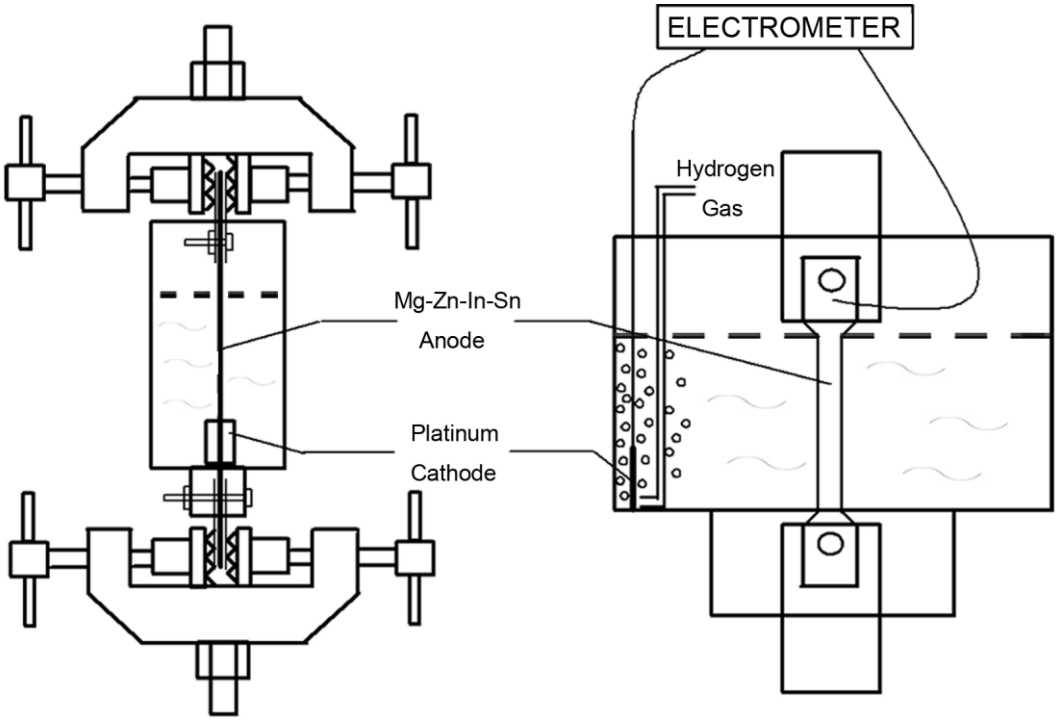

Figure 2. Schematic illustration of stress corrosion apparatus

The electrochemical measurements were carried out in 3.5 wt.% NaCl solution at room temperature. For all the measurements a two electrode electrochemical cell was used, with Mg-Zn-In-Sn alloy anode and standard hydrogen cathode. Excessively large applied stress would easily result in stress corrosion cracking. Therefore, the voltage and current curves of Mg-Zn-In-Sn alloy anode were measured with non-stress corrosion and stresses corrosion of 5, 10, 50, and 100 MPa, all which are in the elastic deformation region of the alloy. The tensile experiments were previously performed with a speed of 300 mm/min (i.e., strain rate 1.9×10^{-1} /s at room temperature), and then electrochemical

measurements were performed with maintaining stresses on alloy anodes using a digital multimeter (Mastech Mas-344).

2.3 Morphological observation and element distribution analysis

After OCP measurements with non-stress and stresses of 5 to 100 MPa corrosion for 1 h, the specimens were cleaned with acetone solution for 5 min using an ultrasonic cleaner (Honda W-113). And then the surface and cross section morphologies of Mg-Zn-In-Sn alloy and the distributions of Mg and oxygen elements on the specimen surface were investigated via SEM (JEOL JSM-5500LV) and EPMA (JEOL JXA-8900R) with an accelerating voltage of 20 V.

2.4 Model calculation

The primary process for the Mg and water is expressed by Equation (1) in 3.5 wt.% NaCl solution:

$$Mg(s) + 2H_2O(l) \rightarrow Mg(OH)_2(s) + H_2(g) \quad (1)$$

The elementary reactions are shown in Table 2. The reaction rate was calculated by the above elementary reactions, and corrosion current model was based on the value of the reaction rate [8]. The corrosion current is assumed independent of fluid flow velocity, which is considered a first-order approximation to the passive current [9]. The LCs were calculated by introducing correction factor A to modify the expression of corrosion current density. Therefore, the LC density was expressed using Equations (2) and (3):

$$i = \frac{[e^{(|E|-E_0)/b_a} - e^{-(|E|-E_0)/b_c}]}{[1/Ai_0 + x]} \quad (2)$$

and

$$x = \frac{e^{(|E|-E_0)/b_a}}{Ai_0 \exp[0.523(|E|-E_0)^5]} \quad (3)$$

where i_0 is the experimental current density, b_a and b_c are the anodic and cathodic Tafel factors, respectively, and E_0 is the equilibrium potential for this reaction, as computed from the Nernst equation. By substituting Equation (3) into Equation (2), the current density is organized into Equation (4).

$$i = \frac{Ai_0 \exp[0.523(|E|-E_0)^5]\{\exp[(|E|-E_0)/b_a] - \exp[-(|E|-E_0)/b_c]\}}{\exp[0.523(|E|-E_0)^5] + \exp[(|E|-E_0)/b_a]} \quad (4)$$

Values for the various parameters are given in Table 3. The LCs density are calculated by modifying the Tafel factors under different stress corrosion conditions of 0 (non-stress), 5, 10, 50, and 100 MPa. Based on Equation (4), the LCs are calculated using Equation (5).

$$I = S \times i \tag{5}$$

where I is the calculation current and S is the surface area of alloy anode. In this paper, the relationship between the stresses and anodic Tafel factors was discussed by comparing calculated values to experimental values.

Table 2. Elementary reactions of Mg alloy anode and water at 25℃

Number	Elementary Reactions
1	$Mg \rightarrow Mg^{2+} + 2e^{-}$
2	$2H_2O + 2e^{-} \rightarrow H_2 \uparrow + 2OH^{-}$
3	$Mg^{2+} + 2OH^{-} \rightarrow Mg(OH)_2 \downarrow$

Table 3. Values for Parameters for the LCs

No.	ip0 (A/m2)	ba (V)	bc (V)	E0 (V)	A
1. 0MPa	0.541	1.690	0.060	-2.37	10
2. 5MPa	0.556	1.720			
3. 10MPa	0.574	1.730			
4. 50MPa	0.617	1.735			
5. 100MPa	0.645	1.740			

3. RESULTS AND DISCUSSION

3.1 Tension properties

Through the tensile test, the mechanical properties of the Mg-Zn-In-Sn alloy could be compared in the rolling and transverse directions. Ultimate tensile strength (UTS)s were 386 and 326 MPa, and strain rates were 9.5% and 4.6% in rolling and transverse directions, respectively, as shown in Table 4. As determined through the tensile test, the tensile strengths in the elastic deformation region ranged from 0 MPa to 200 MPa. Based on the above results, the applied stresses were set to 0 (non-stress), 5, 10, 50 100 MPa during the stress corrosion experiments in this paper.

Table 4. Values of ultimate tentile strengh (UTS) and elongation for Mg-Zn-In-Sn alloy

Mg-Zn-In-Sn alloy	Strain rate	UTS(MPa)	Elongation(%)
Rolling direction	ε=5×10-5/s	386	9.5
Transverse direction		326	4.6

3.2 Electrochemical measurements

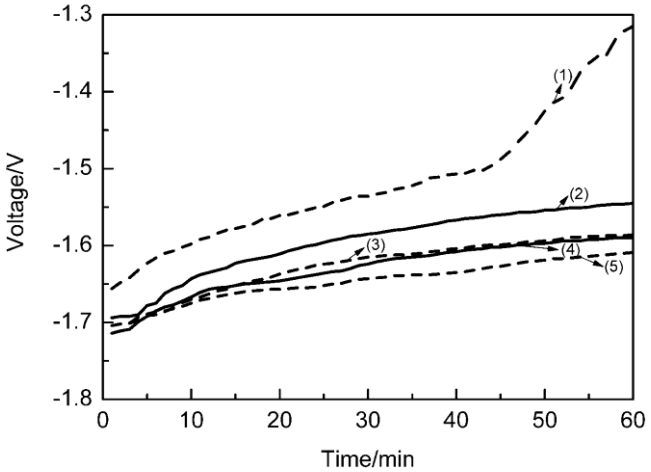

Figure 3. OCP of Mg-Zn-In-Sn alloy anode under stress corrosion (1) 0 MPa; (2) 5 MPa; (3) 10 MPa; (4) 50 MPa; (5) 100 Mpa

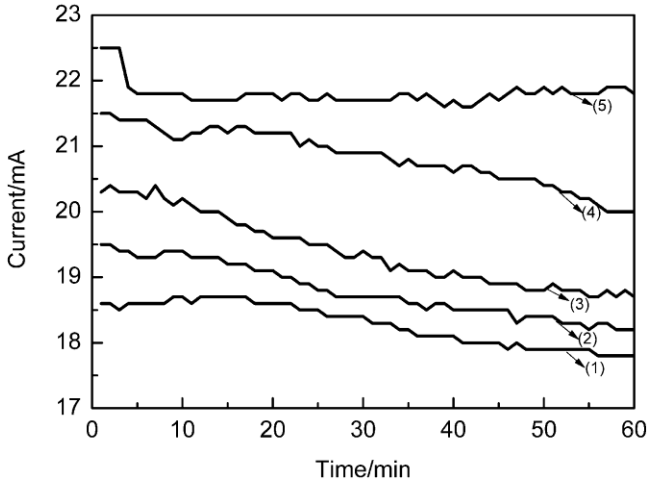

Figure 4. LC of Mg-Zn-In-Sn alloy anode under stress corrosion (1) 0 MPa; (2) 5 MPa; (3) 10 MPa; (4) 50 MPa; (5) 100 Mpa

Figures 3 and 4 show the OCPs and LCs of the Mg-Zn-In-Sn alloy anode with non-stress corrosion and stresses of 5 to 100 MPa. These results indicate that Mg-Zn-In-Sn alloy anode with stress of 100 MPa featured the most negative voltage and the highest current. The applied stress energy improved the electrochemical potentials of alloy anode, and persisted together with stresses, because

the stresses did not exceed the elastic limit. The change in free energy ΔG (per g) is given by Equation (6):

$$\Delta G = \frac{\sigma^2}{2\rho Y} \tag{6}$$

where σ is the applied stress, Y is Young's modulus, and ρ is the density of the Mg-Zn-In-Sn alloy. The free energy of Mg-Zn-In-Sn alloy anode increased as the applied stresses increased. The negative removal of voltage ΔE was calculated with the change in energy using Equation (7).

$$\Delta E = -\frac{\Delta G}{nF} \tag{7}$$

where n is the number of moles of electrons transferred and F is the Faraday constant. As the energy increased, the OCPs of the alloy anodes were negatively removed [10].

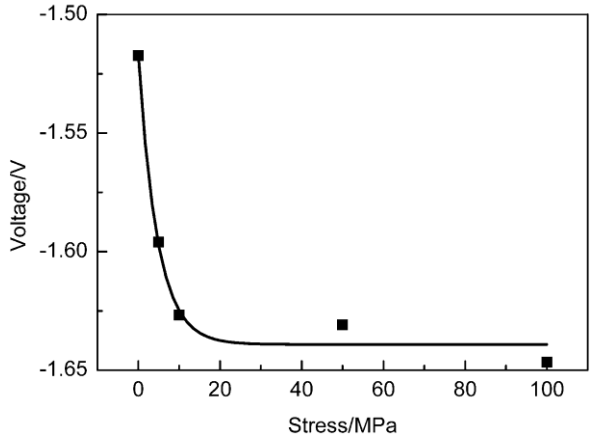

Figure 5. Average OCP-stress curve

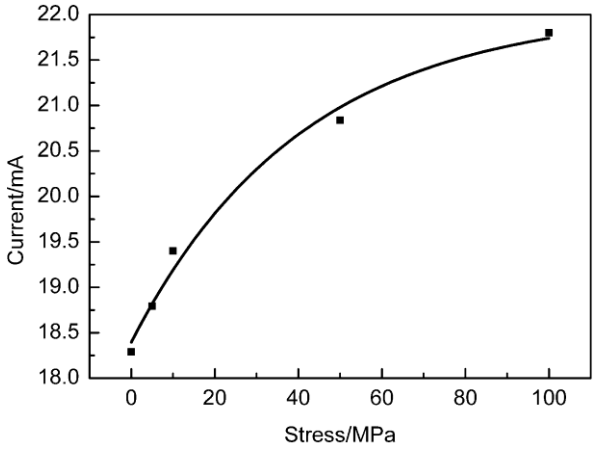

Figure 6. Average LC-stress curve

The OCP of alloy anode with non-stress occurred at a significantly positive move at approximately 40 min, as shown in Fig. 3. This result can be attributed to the gradually forming of corrosion product film, which hindered the corrosion reaction between Mg-Zn-In-Sn alloy anode and NaCl solution. The OCPs of alloy anode had apparently negative removals with increasing of stresses below 10 MPa. However, no evident changes in the OCPs were observed with the increasing of stresses from 10 to 100 MPa. The experimental results are not exactly consistent with the analyzed results according to the applied energy because of the resistance of corrosion product films, which are discussed later in this paper. As shown in Fig. 6, the average LCs of Mg-Zn-In-Sn alloy anode improved as the applied stresses increased because of increasing of the micro surface area of alloy anodes [11]. Therefore, negative OCPs and high LCs of alloy anode were obtained by effect of stress.

3.3 Morphologies of Mg-Zn-In-Sn alloy anodes after OCP measurements

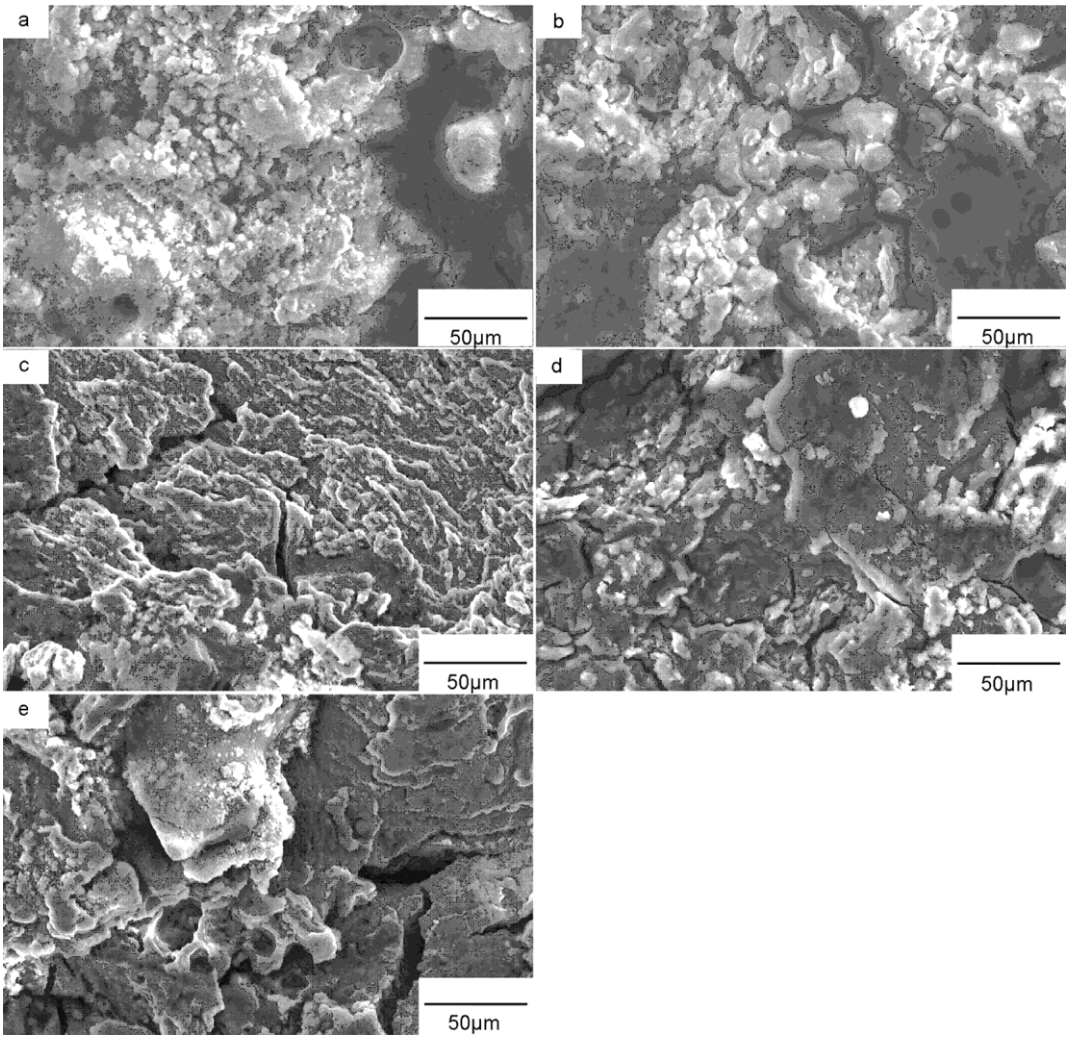

Figure 7. SEM image of stress corrosion surface morphology (a) 0 MPa; (b) 5 MPa; (c) 10 MPa; (d) 50 MPa; (e) 100 MPa

The surface and cross section morphologies of alloy anode were observed after OCP measurement experiments with non-stress corrosion and stresses corrosion of 5 to 100 MPa were performed for 1 h. The surface morphology of specimen with non-stress was uniformly covered with the corrosion product film as shown in Fig. 7a. The corrosion reaction between alloy anode and NaCl solution was hindered by forming of the film. Therefore, the OCPs of alloy anodes had an apparently positive removal as experiment progressed. However, applied stresses promoted electrochemical activities of alloys, the corrosion product films on the specimens became easy to shed off as shown in Figs. 7b–7e.

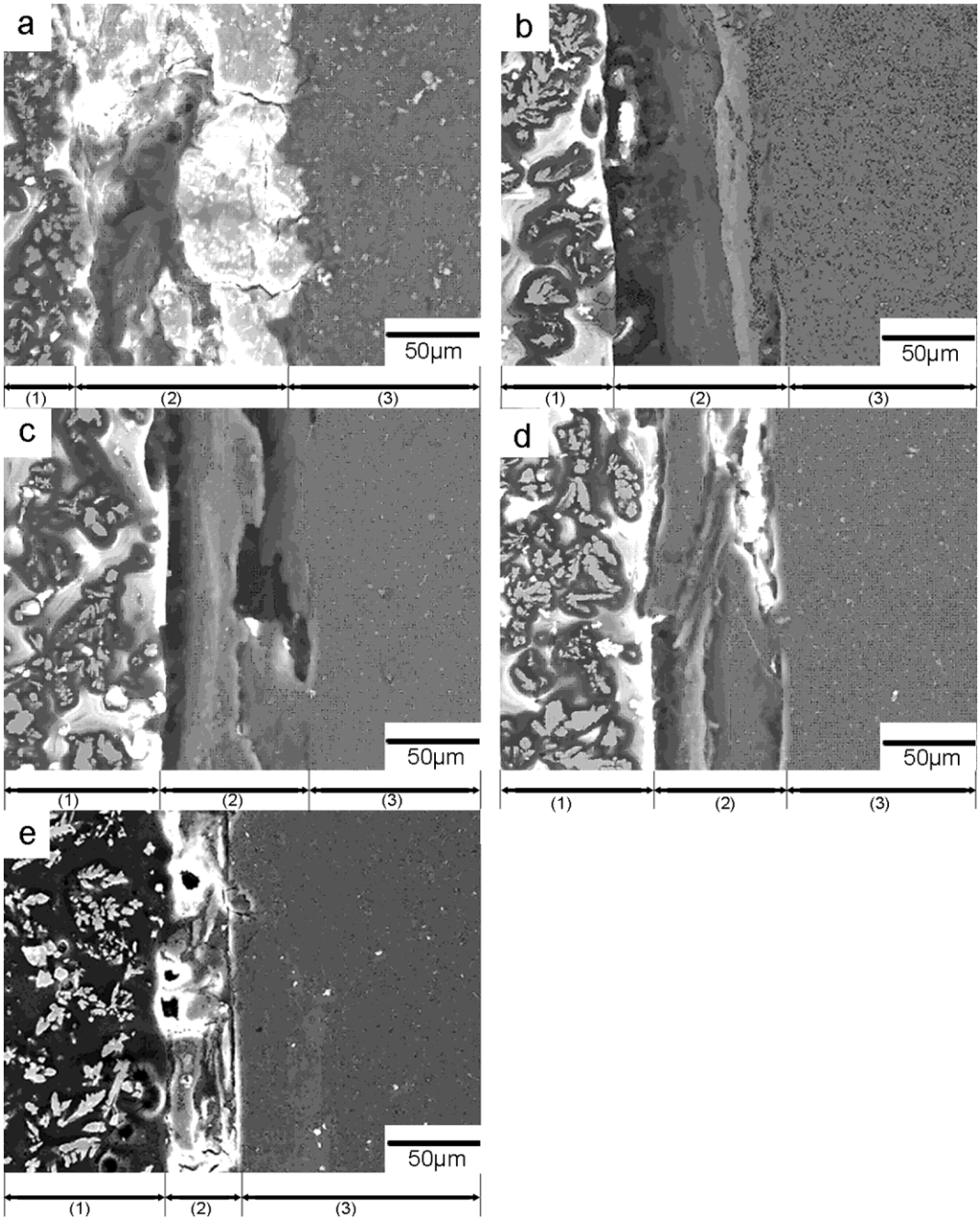

Figure 8. SEM image of stress corrosion cross section morphology (1) conductive resin, (2) corrosion product layer, (3) alloy matrix (a) 0 MPa; (b) 5 MPa; (c) 10 MPa; (d) 50 MPa; (e) 100 MPa

The resistance between NaCl solution and alloy anode decreased, which promoted the electrochemical corrosion reaction. As shown in Fig. 7b, the surface of alloy anode was almost covered with the corrosion film with a few light cracks. Therefore, the OCP with stress of 5 MPa was a little higher than that with non-stress. As shown in Figs. 7c–7e, the corrosion product films were shed off intensively by the effect of stresses, and numerous cracks appeared on the films. The OCPs of alloy anodes had apparently negative removals as the applied stresses increased.

Figures. 8a–8e show the cross section morphologies of alloy anodes after OCP measurements with a conductive resin on the left-hand side, the corrosion product film in the middle and not corroded part of the alloy matrix on the right-hand area . The thickness of corrosion product film was approximately 80 μm with non-stress (Fig. 8a). The thickness of the film decreased to approximately 50 μm with the applied stress of 5 MPa (Fig. 8b). Subsequently, the thickness of the film deceased to 30 μm and did not change significantly with stresses of 10, 50, and 100 MPa, as shown in Figs. 8c–8e. This result indicates that the thicknesses of corrosion product films decreased apparently by effect of stresses. Therefore, the electrochemical corrosion reactions between Mg-Zn-In-Sn alloy and NaCl solution progressed smoothly, and higher electrochemical potential of alloy anode could be obtained by stress corrosion. However, with stresses of 10, 50, and 100 MPa, the thicknesses of the corrosion product films had no evident changes with the increasing of stresses. The OCP values had no significantly negative removal with these stresses, neither, as discussed in the above results. The OCP results variation is well consistent with the changing of corrosion product film thicknesses. The variation of OCP results are demonstrated by the observation of cross section morphologies.

3.4 Element distribution of the Mg-Zn-In-Sn alloy after OCP measurements

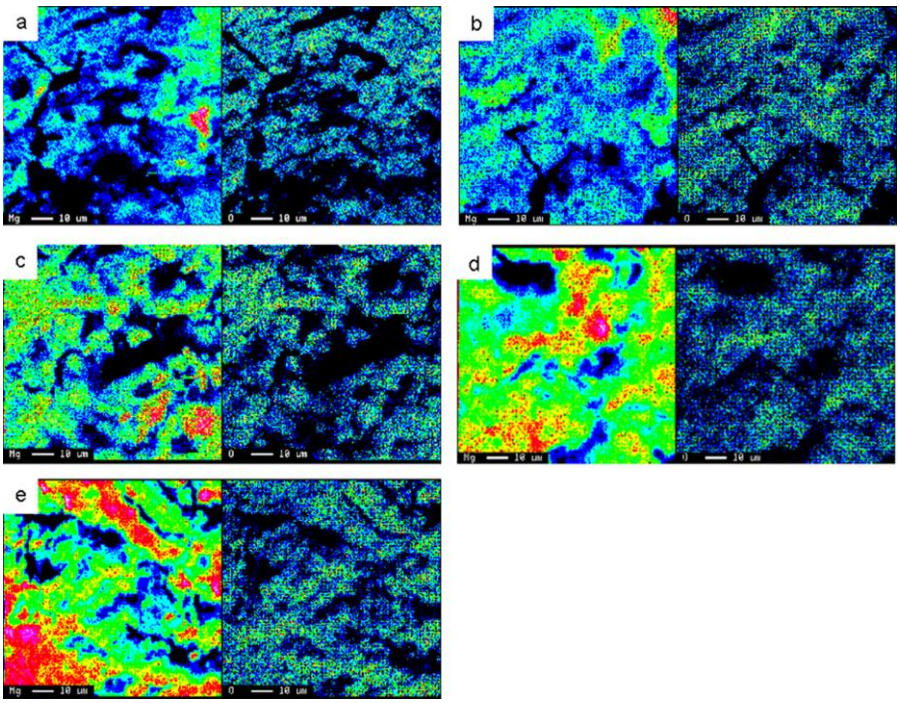

Figure 9. EPMA image of stress corrosion surface morphology (a) 0 MPa; (b) 5 MPa; (c) 10 MPa; (d) 50 MPa; (e) 100 MPa

The Mg and oxygen elements distribution on the surface of Mg-Zn-In-Sn alloy anodes are shown in Fig. 9, which were performed with OCP measurements for 1 h with non-stress and stresses of 5 to 100 MPa. As shown in Fig. 9a, Mg and oxygen elements uniformly distribute on the surface of specimen. However, the black part appears in the picture due to the uneven surface of corrosion product film. This result indicates alloy anode surface was continuously covered with the corrosion product film. But the ratios of Mg element gradually increased with stressed of 5 MPa to 100 MPa as shown in Figs. 9b–9e. The continuous corrosion product films covered on specimen surface were easy to shed off and the thickness of films decreased apparently by applied stresses. Therefore, the effect of stresses was investigated to increase the ratios of Mg element on the surface of specimen corroded, which contributed the reaction between Mg-Zn-In-Sn alloy and NaCl solution to occur more easily.

3.5 Model calculation of current curves

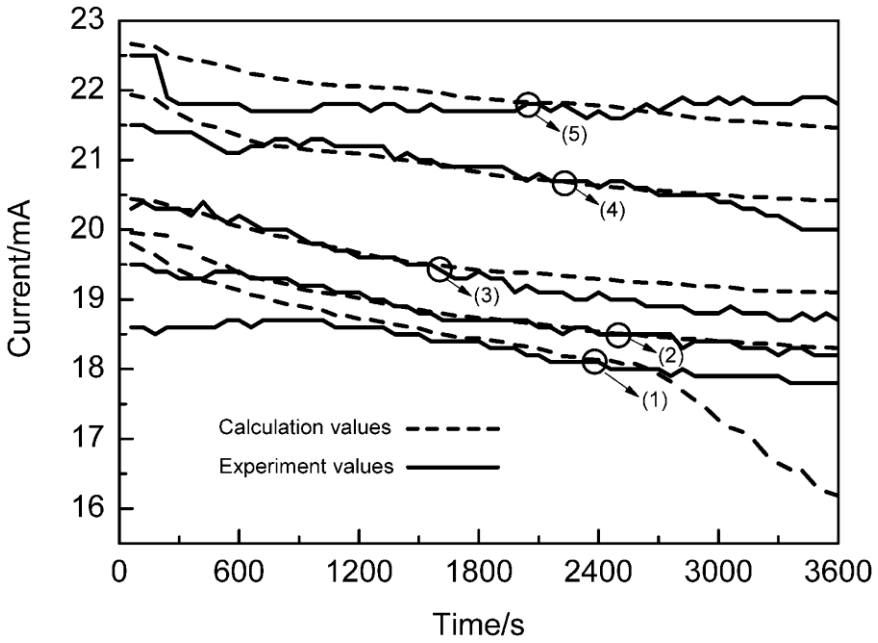

Figure 10. Comparison of LC curves for Mg-Zn-In-Sn alloy anode under stress corrosion (1) 0 MPa; (2) 5 MPa; (3) 10 MPa; (4) 50 MPa; (5) 100 MPa

Equations (6) and (7) were developed empirically and provide a reasonable representation of experimental results. By adjusting the Tafel factors, the calculated results were mainly consistent with the experimental results. Comparisons of the current curves between experimental and calculated values are shown in Fig. 10. Therefore, as shown in Table 4, the stresses have effects on the changes in the anodic Tafel factors. The Tafel factors become bigger as stresses increased, and the LC values also improved as the Tafel factors increased. The modified model of the LC verifies the reliability of experimental results. However, the calculated results were not exactly consistent with experimental results. This finding can be attributed to the interference of environmental factors, such as the forming of corrosion product film and pH value of solution [4, 12].

4. CONCLUSIONS

This paper determined the effects of stress on the electrochemical properties of Mg-Zn-In-Sn alloy anode through electrochemical property measurements, morphological observations, and element distribution analysis. Furthermore, the LCs were calculated by the modified model of corrosion current density, in order to reveal the relation of stress and Tafel factor.

1. The Mg-Zn-In-Sn alloy anode with stress of 100 MPa exhibited a negative OCP (-1.647 V) and a high LC (21.802 mA).

2. The OCPs of alloy anodes were improved as the applied energy increased. And LCs of Mg-Zn-In-Sn alloy anode improved as the applied stresses increased because of increasing of the micro surface area of alloy anodes.

3. The corrosion product films on the surface of specimen became easy to shed off due to the applied stresses. The resistance between NaCl solution and alloy anode decreased, which promoted the electrochemical corrosion reaction.

4. In general, the thicknesses of corrosion product films on alloy anodes surface decreased as the applied stresses increased. However, the thicknesses of corrosion product films with stresses above 10 MPa did not decrease significantly. This phenomenon explains the variation of OCP values of alloy anode because of the influence of experimental factors.

5. The effect of stresses was investigated to increase the ratios of Mg element on the surface of specimen corroded, which contributed the reaction between Mg-Zn-In-Sn alloy and NaCl solution to occur more easily.

6. By adjusting the Tafel factors, the calculated results of LC were mainly consistent with the experimental results. The infuence of stresses on the LC was revealed on the theoretial.

ACKNOWLEDGEMENTS
The present research is partially supported by the Open-Research Center in Saitama Institute of Technology in Japan.

References

1. X. D. Hu, “Studies on strip casting and rolling of magnesium alloy thin strip” (PH.D. Thesis, Saitama University, Japan, 2007).
2. T. D. Gregory, R. J. Hoffman, and R. C. Winterton, *J. Electrochem. Soc*. 137 (1990): 775.
3. Z. Yu, D. Y. Ju, H. Y. Zhao, and X. D. Hu, *J. Environ. Sci*. 23 (2011): 95.
4. P. L. Bonora, M. Andrei, A. Eliezer, E. M. Gutman, *Corr. Sci*. 44 (2002): 729.
5. W. Walke, J. Przondziono, E. Hadasik, J. Szala, D. Kuc, *J. Achievements Mater. Manufact. Engin*. 45 (2011): 132.
6. A.Eliezer, *Adv. Mater. Res*. 95 (2010): 79.
7. Z. Yu, H. Y. Zhao, X. D. Hu, D. Y. Ju, *Transactions of Nonferrous Metals Society of China*. 20 (2010): 318.
8. K. Ishigure, T. Nukii, S. Ono, *J. Nuclear Mater*.. 350 (2006): 56.
9. D. D. Macdonald, *Corr. Sci*. 48 (1992): 194.
10. M. Clarke, *Corr. Sci*. 10 (1970): 671.

11. T. Shibata, *Journal of the Society of Materials Science*. 55 (2006): 979.
12. Y. B. Unigovski, L. Riber, E. M. Gutman, *Journal of Metals, Materials and Minerals*. 17 (2007): 7.